Structural and Multidisciplinary Optimization (2021) 63:39–58
https://doi.org/10.1007/s00158-020-02771-5

RESEARCH PAPER

Topological constraints in 2D structural topology optimization

Haitao Han[1,2] · Yuchen Guo[1,2] · Shikui Chen[3] · Zhenyu Liu[1]

Received: 17 September 2019 / Revised: 22 August 2020 / Accepted: 26 October 2020 / Published online: 17 November 2020

Abstract

One of the straightforward definitions of structural topology optimization is to design the optimal distribution of the holes and the detailed shape of each hole implicitly in a fixed discretized design domain. However, typical numerical instability phenomena of topology optimization, such as the checkerboard pattern and mesh dependence, all take the form of an unexpected number of holes in the optimal result in standard density-type design methods, such as SIMP and ESO. Typically, the number of holes is indirectly controlled by tuning the value of the radius of the filter operator during the optimization procedure, in which the choice of the value of the filter radius is one of the most opaque and confusing issues for a beginner unfamiliar with the structural topology optimization algorithm. Based on the soft-kill bi-directional evolutionary structural optimization (BESO) method, an optimization model is proposed in this paper in which the allowed maximal number of holes in the designed structure is explicitly specified as an additional design constraint. The digital Gauss-Bonnet formula is used to count the number of holes in the whole structure in each optimization iteration. A hole-filling method (HFM) is also proposed in this paper to control the existence of holes in the optimal structure. Several 2D numerical examples illustrate that the proposed method cannot only limit the maximum number of holes in the optimal structure throughout the whole optimization procedure but also mitigate the phenomena of the checkerboard pattern and mesh dependence. The proposed method is expected to provide designers with a new way to tangibly manage the optimization procedure and achieve better control of the topological characteristics of the optimal results.

Keywords Topological constraints · Topological optimization · Digital Gauss-Bonnet formulation · Burning method

1 Introduction

Topological optimization is one of the design methods used to determine material distribution in a specified domain. Currently, it has been extended to the areas of structural mechanics (Lazarov et al. 2016; Sigmund 2009; Rozvany 2001; Chen et al. 2010), electromagnetism (Deng and Korvink 2018; Okamoto et al. 2016; Labbe and Dehez 2011), thermology (Sigmund 2001b, c), and fluid mechanics (Deng et al. 2011; Gersborg-Hansen et al. 2005; Evgrafov et al. 2008; Borrvall and Petersson 2003), among others.

However, in the standard density-type design methods, there still exist various typical numerical instability phenomena, such as the checkerboard pattern and mesh dependence, resulting from the emergence of many holes. Hence, these phenomena are typical problems in topological optimization that have been widely studied (Sigmund and Petersson 1998; Guest et al. 2004; Rozvany 2009; Bourdin 2001; Buhl et al. 2000; Yamada et al. 2010; Talischi et al. 2012; Zuo and Saitou 2017).

This paper proposes a new method named the hole-filling method (HFM) to mitigate the phenomena of the checkerboard pattern and mesh dependence by constraining the number of holes in a topological structure obtained in each iteration of topological optimization. The general idea of the HFM is to fill in the extra holes generated during iterative optimization. Consequently, the peak in the number of holes that arise during the topology optimization process is constrained to be fewer than or equal to a certain allowed maximum number of holes in the HFM. The mesh dependence phenomenon can be controlled when the allowed maximum number of holes in the

Responsible Editor: Ji-Hong Zhu

Supplementary Information The online version contains supplementary material available at https://doi.org/10.1007/s00158-020-02771-5.

Zhenyu Liu
liuzy@ciomp.ac.cn

1 Changchun Institute of Optics, Fine Mechanics and Physics (CIOMP), Chinese Academy of Sciences, Changchun 130033, China

2 University of Chinese Academy of Sciences, Beijing 100049, China

3 Department of Mechanical Engineering, State University of New York, Stony Brook, USA

optimal structure (H) is set to an appropriate value. Moreover, because the checkerboard pattern corresponds to the formation of regions of alternating solid and void elements ordered in a checkerboard-like fashion, this phenomenon can also be successfully suppressed by filling in holes of unit area in the optimal structure with the HFM.

The HFM proposed in this paper is based on the soft-BESO method (Huang and Xie 2009, Xie and Steven 1992) of solving topology optimization problems while controlling the number of holes. Although the SIMP method (BendsØe 1989; Bendsøe and Sigmund 1999, Zhou and Rozvany 1991; Mlejnek 1992; Sigmund 2001a; Andreassen et al. 2011), the level set method (Osher and Sethian 1988), and the ESO method (Xie and Steven 1992) have all been widely used for structural topology optimization, the ESO method is chosen for the following reasons. The level set method introduces a function with one more dimension than the design domain and determines the boundary of the structure using the zero-level set of this function. The maximum number of holes during the optimization procedure is limited by the initial value of the setup of level set surface in a two-dimensional case. Hence, the level set method is out of the scope of this article. The SIMP method and the ESO method are both density-type methods. However, the original digital Gauss-Bonnet theorem requires clear boundaries between solid elements and void elements. During the optimization process of the SIMP method, grey-type domains exist at the boundaries between solid domains and void domains. Because this article focuses on the method of controlling holes rather than the binarization of continuous variables, the SIMP method is also out of the scope of the current study.

The ESO method was proposed by Xie and Steven in the early 1990s and has been applied to a large number of topological optimization problems (Xie and Steven 1997). The soft-kill BESO method, one of the extensions of the ESO method, has the characteristic of binarization of the solution obtained in each optimization iteration. This is a necessary condition for the implementation of the digital Gauss-Bonnet theorem for closed digital surfaces.

The proposed HFM is a method that can fill in holes in a solid domain. Therefore, the HFM method can restrict the number of holes in an optimal structural design in two-dimensional space. Although the filter scheme (Sigmund 2007; Bourdin 2001; Wang et al. 2011; Lazarov and Sigmund 2011) also influences the number of holes and offers a straightforward way to control the number of holes in the optimal structure, it has the following disadvantages: (a) there is no general rule governing the mapping between the number of holes in the optimal structure and the filter radius size; (b) a large filter radius may change the optimal topology by causing thin parts of the structure to be filtered out; and (c) the choice of the filter radius size is not straightforward for a designer who is not already familiar with topology optimization.

The rest of this paper is organized as follows. Section 2 introduces the topology optimization problem with a constraint on the number of holes in the optimal structure as well as the underlying theory, the implementation details, and the flow chart of the HFM. Section 3 presents the numerical implementation results for typical cantilever beams with different parameters. Section 4 discusses the HFM. Section 5 offers further discussions and suggests possible directions of future research. Section 6 offers a statement regarding the replication of the results.

2 The hole-filling method

2.1 Soft-kill BESO topology optimization model with HFM

The aim of topology optimization is to find an optimal distribution of material, i.e., the implementation of the minimal compliance, subject to constraints on the volume of the material and an allowed maximum number of holes. The method presented in this paper is based on the soft-kill BESO method. The design domain is assumed to be rectangular and discretized into square finite elements in the horizontal (xh: the numbers of elements in this direction) and vertical (yv: the numbers of elements in this direction) direction. The Young's modulus is interpolated from the element density design variable as follows:

$$\mathrm{E_e}(\mathrm{x_e}) = \mathrm{E_1}\rho_\mathrm{e}^\mathrm{p} \tag{1}$$

where $\mathrm{E_1}$ is the Young's modulus of the solid material and p is the penalization power. The control of the allowed maximum number of holes is implemented as a constraint in the topology optimization problem. In this paper, the topology optimization problem can be expressed as (2-a) and (2-b):

$$\begin{aligned}
&\min_{\rho} : \mathrm{c}(\boldsymbol{\rho}) = \sum_{e=1}^{N} \frac{1}{2}\rho_\mathrm{e}{}^\mathrm{p}\left(\mathbf{u_e}{}^\mathrm{T}\mathbf{k}_0\mathbf{u_e}\right) && (2-\mathrm{a})\\
&\mathrm{s.t.} : \mathrm{V}^* - \textstyle\sum_{e=1}^{N}\mathrm{V_e}\rho_e = 0\\
&\qquad \mathbf{KU} = \mathbf{F}\\
&\qquad \rho_e = \{\rho_{\min}, 1\}\\
&\qquad \mathrm{h} \leq \mathrm{H}
\end{aligned}$$

$$\begin{aligned}
&\min_{\rho} : \ \mathrm{c}(\boldsymbol{\rho}) = \sum_{e=1}^{N} \frac{1}{2}\rho_\mathrm{e}{}^\mathrm{p}\left(\mathbf{u_e}{}^\mathrm{T}\mathbf{k}_0\mathbf{u_e}\right) && (2-\mathrm{b})\\
&\mathrm{s.t.} \ : \ \mathrm{V}^* - \textstyle\sum_{e=1}^{N}\mathrm{V_e}\rho_e = 0\\
&\qquad \mathbf{KU} = \mathbf{F}\\
&\qquad \rho_e = \{\rho_{\min}, 1\}\\
&\qquad \mathrm{h} \leq \mathrm{H}\\
&\qquad \mathrm{S_i} > \mathrm{S}^*
\end{aligned}$$

where c is the optimization objective; **U** is the global displacement; **F** is the force vector; **K** is the global stiffness matrix; $\mathbf{u_e}$ is the element displacement vector; $\mathbf{k_0}$ is the element stiffness matrix for an element with unit Young's modulus; $\boldsymbol{\rho}$ is the vector of design variables; N (= xh×yv) is the number of elements used to discretize the design domain; V_e is the volume of an individual element (in this paper, $V_e = 1$); ρ_e is the design variable for the e-th element; V^* is the prescribed volume of the final structure; h is the number of holes in the structure obtained in each optimization iteration; H is the allowed maximum number of holes in the structure; S_i is the area of the i-th hole; and S^* is a prescribed value of minimum area of the hole in final structure. In this paper, we only discuss the following two cases: without controlling area of holes (based on the optimization model in (2-a)) and controlling area holes lager than 1 (based on the optimization model in (2-b)).

2.2 Calculation of the number of holes in a structure in 2D

Before counting the number of holes, the definition of a hole in two-dimensional discretized space should be clarified. In this paper, a hole is considered to be formed by a closed digital curve composed of the edges of several solid square elements, as shown in Fig. 1, where neither (a) nor (c) is a hole but (b) is a hole.

According to the Gauss-Bonnet theorem for closed digital surfaces in 3D digital space (Chen and Rong 2010 and Chen 2004), the genus g of a closed digital surface can be expressed in terms of the properties of a set of digital points. A two-dimensional digital space can be treated as a simplified three-dimensional digital space with only one layer of square elements on the *x-y* plane, as shown in Fig. 2. With this precondition, the genus number of a three-dimensional structure is equal to the number of holes in the corresponding two-dimensional structure. Thus, the formula for g in a 2D digital space can be expressed as follows:

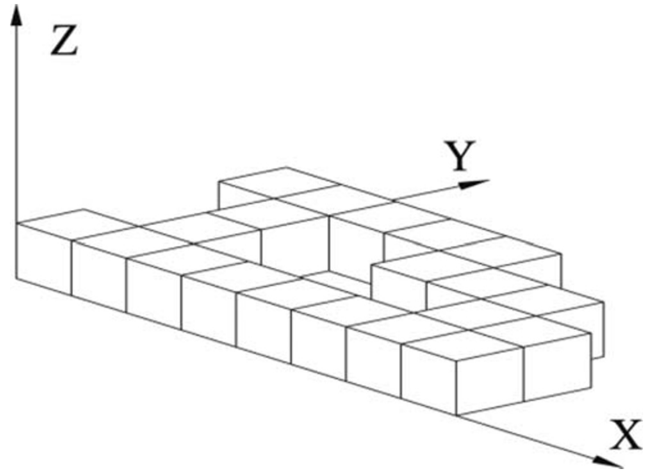

Fig. 2 A three-dimensional digital structure with only one layer of square elements, corresponding to the two-dimensional digital spatial structure shown in Fig. 1

$$g = 1 + \frac{|M_4| - |M_2|}{4} \tag{3}$$

where g is the number of holes in the connected structure and the M_i (i = 4, 2) are sets of digital points on the boundary of the solid structure. A digital point represents a connection among multiple edges of solid elements, where the number of connected edges is i, as shown in Fig. 3. For the example of M_4 shown in Fig. 3b, $|M_4| = 2$.

However, during the topological optimization process using the BESO method, one structure may have multiple separate parts, in which case the Gauss-Bonnet formulation is not suitable. Therefore, the formulation must be changed as follows:

$$\mathrm{h} = n + \frac{|\mathrm{M}_4| - |\mathrm{M}_2|}{4} \tag{4}$$

where n is the number of connected structures in the current iteration of topology optimization and is calculated as

Fig. 1 Neither (**a**) nor (c) is a hole; (**b**) is a hole

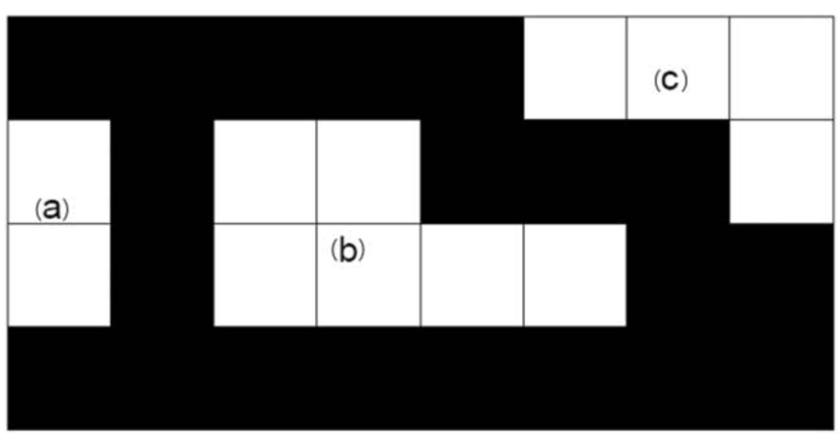

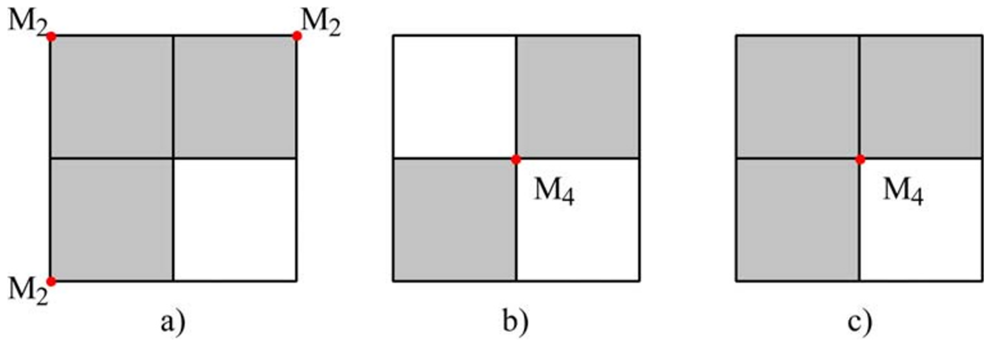

Fig. 3 The cases of M_2 (**a**) and M_4 (**b**, **c**). The solid elements are shown in grey, the edges of each element are shown in black, and the hole elements are shown in white

follows. Consider multiple sets A_i, each representing one singular connected structure that consists of solid elements; then, a set B that consists of the solid elements of all connected structures can be expressed in terms of the sets A_i as follows:

$$B = \overset{n}{\underset{i=1}{\cup}} A_i \text{ and } \overset{n}{\underset{i=1}{\cap}} A_i = \varnothing \quad (5)$$

The key to solving this formula (5) is to find the corresponding set of solid elements of a connected structure that exactly fits the concept of the burning method (Gu and Yau 2008). Given a virtual fire point, the fire will spread such that the boundary of the burning area will gradually expand until it reaches an incombustible boundary. In Fig. 4, the detailed process is illustrated. The steps of the process are listed as follows:

(a). Let all of the solid elements constitute a set B; choose a solid element b_1 from B.
(b). Find the elements constituting the set C connected to solid element b_1 by a shared edge and point.
(c). Select the elements from C that are also solid elements in B to construct a set D, and then clear set C.
(d). Let the elements of D and b_1 together constitute set A_1.
(e). Remove the elements in D from the solid element set B, and then find the elements that constitute a new set C connected to any of the solid elements in D by a shared edge and point.
(f). Repeat Steps (c), (d) and (e) until the set C contains no elements that are included in B, and then clear set D; the set A_1 thus obtained is a connected structure.

All Steps (a), (b), (c), (d), (e), and (f) are repeated until the set B contains no elements and (5) has been solved. Thus, the number of holes h (in (4)) is obtained in each iteration of the topology optimization process.

2.3 Calculation of the areas of all holes in a topological structure

Since the elements of a hole that are connected to each other can be identified by checking whether void elements share edges, the calculation of the areas of all holes in a topological structure in two-dimensional digital space is similar to the calculation of the number of connected structures. Thus, the burning method is used again. The steps are listed as follows:

a) Let all of the void elements constitute a set VB; choose a void element vb_1 from VB.
b) Find the elements that constitute the set VC connected to void element vb_1 by a shared edge.

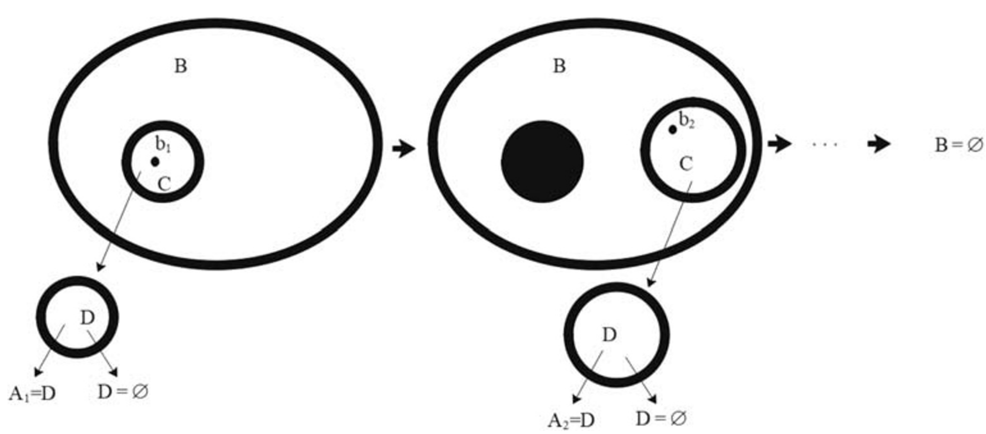

Fig. 4 The relationship diagram of the process of the burning method

c) Select the elements from VC that are also void elements in VB to construct a set VD, and then clear set VC.
d) Let the elements of VD and vb_1 together constitute set VA_1.
e) Remove the elements in VD from the void element set VB, and then find the elements that constitute a new set VC connected to any of the void elements in VD by a shared edge.
f) Repeat Steps (c), (d), and (e) until the set VC contains no elements that are also included in VB, and then find the elements that constitute the set VC connected to any of the void elements in VD by a shared edge. If any element exists in VC that does not belong to the design domain, then the void elements do not belong to a hole; clear sets VD and VA_1. Otherwise, the set VA_1 is a hole.

All Steps (a), (b), (c), (d), (e), and (f) are repeated until the set VB contains no void elements. Then, the cell {VA} is an ordered set of the areas of all holes.

2.4 Implementation of the HFM

According to the underlying principle of the HFM, the implementation of hole number control requires two essential components: (i) the number of holes h in the topological structure in each iteration of topology optimization and (ii) an ordered set of the areas of all holes in the topological structure in each iteration of topology optimization.

Both of these essential components have been obtained in Sections 2.2 and 2.3. The next step is to control the number of holes. The allowed maximum number of holes in the topological structure in each iteration of topological optimization is considered a constraint in the optimization problem (2).

Because the area of a hole S_i can be calculated as the number of elements in which the density variable ρ_e is equal to ρ_{min}, a large hole contains more minimal density variables than a small hole. Heuristically, in the optimization procedure, we assume that filling in a smaller hole with solid material will cause a smaller change in the value of the optimization objective than filling in a larger one. Because the topology optimization process of the BESO method begins from an initial state in which the number of holes in the structure is zero, the inequality constraint $h \leq H$ is always satisfied at the beginning of optimization. With the evolution of structural optimization, the areas of newly generated holes are calculated, and the smallest holes will be filled in if the inequality constraint $h \leq H$ is violated. Therefore, the idea of the HFM is to fill in a relatively small hole when the number of holes in the current iteration of topology optimization is greater than the allowed maximum number of holes (H). The holes in a structure can be arranged in order from the largest to the smallest based on their areas. The formulation of the HFM is expressed as follows:

$$\rho_e = \begin{cases} \rho_e, h \leq H \\ 1, \quad h > H, \rho_e \in \left\{ G_j | G_{j-1} > G_j, h-H \leq j \right\} \end{cases} \tag{6}$$

where G is the cell of the holes ranked in area from largest to smallest, consisting of finite elements, and j represents the position in the cell G corresponding to the hole with the j-th largest area; hence, G_j represents the j-th hole. Thus, the number of holes in the topological structure in each iteration of topological optimization can be kept within the allowed range.

2.5 Checkerboard pattern and mesh dependence

The checkerboard pattern is one type of numerical instability phenomena, which are typically solved by using filters for sensitivity or density variables. In the case that the design domain is discretized into square elements of unit length, the checkerboard pattern can be phenomenologically treated as corresponding to holes with an area of 1. Theoretically, the area of each hole can be obtained in the HFM, thus making it possible to suppress holes with a specific area value. Hence, holes of unit area in the optimal structure will be filled in by default in the HFM. Because the checkerboard pattern corresponds to the formation of regions of alternating solid and void elements ordered in a checkerboard-like fashion, this phenomenon can be prevented by automatically filling in holes of unit area.

The primary function of the HFM is to control the number of holes to be fewer than or equal to the maximum number of holes H. It is theoretically possible to choose an appropriately small value of H to maintain mesh independence. The reason for this is that reasonable optimal structures inherently have both a lower bound and an upper bound on the number of holes they can contain. H is such an upper bound. As the upper bound H decreases, the range of the possible number of holes in the optimal structure will be restricted. Therefore, the HFM may mitigate the phenomenon of mesh dependence.

2.6 Flow chart of optimization with the HFM

The iterative topology optimization procedure of the proposed HFM is described as follows:

a) Discretize the design domain using a finite element mesh, and assign initial parameters for the topology optimization program.

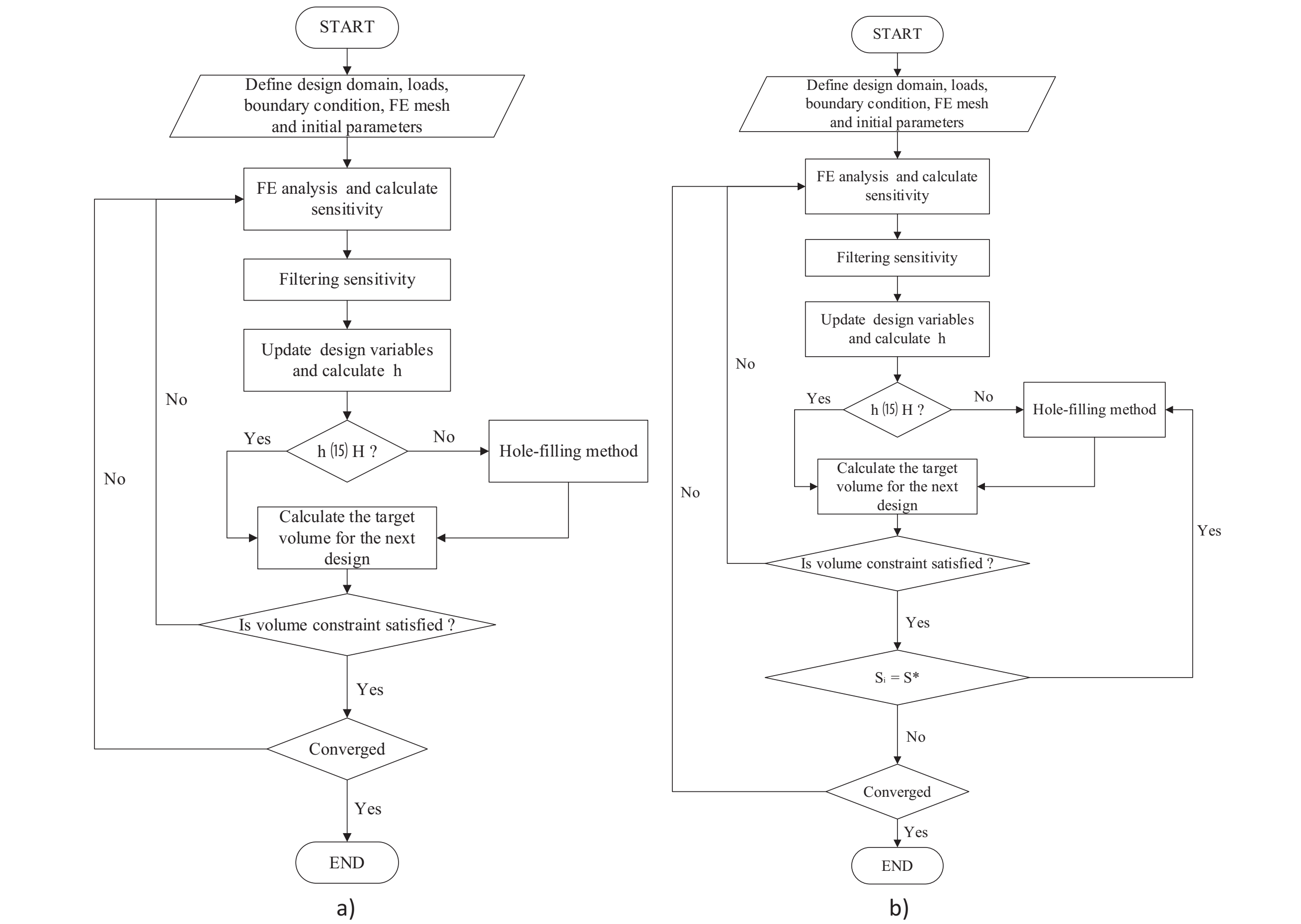

Fig. 5 Flow chart of the optimization process with the HFM corresponds to **a** topology optimization model in (2-a) and **b** topology optimization model in (2-b)

b) Perform finite element analysis (FEA), and then calculate the elemental sensitivity number according to the original BESO method.
c) Apply a filter module to filter based on the elemental sensitivity number.

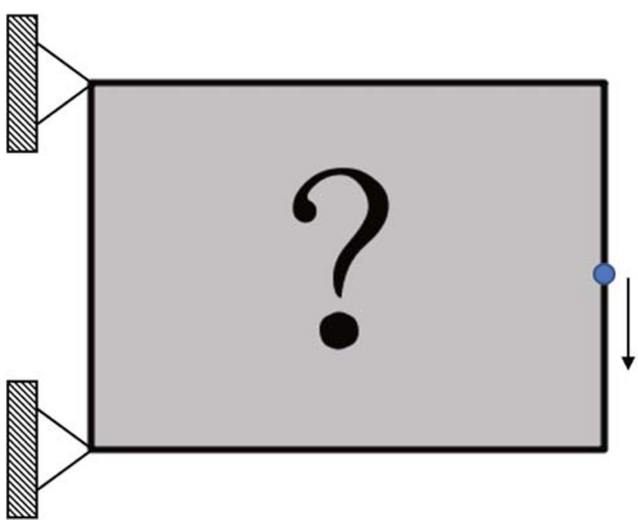

Fig. 6 A cantilever beam with a right-middle point force

d) Update the design variables and then calculate the number of holes h in the topological structure.
e) Determine whether the number of holes satisfies the constraint $h \leq H$. If $h \leq H$, proceed to Step f; otherwise, apply the HFM and then proceed to Step f.
f) Calculate the target volume for the next design. If the volume of the structure satisfies the volume constraint, determine whether any holes of unit area exist in the structure. If so, apply the HFM to fill them; otherwise, determine whether the program meets the convergence criterion.

Steps b–f are repeated until the program meets the convergence criterion. The program flow chart is shown in Fig. 5.

3 Numerical examples

In this section, several numerical examples are presented to illustrate the working principle of the HFM and its ability to suppress the checkerboard pattern and mesh dependence phenomena. Section 3.1 demonstrates the essential function of the HFM, which is to control the number of holes, under

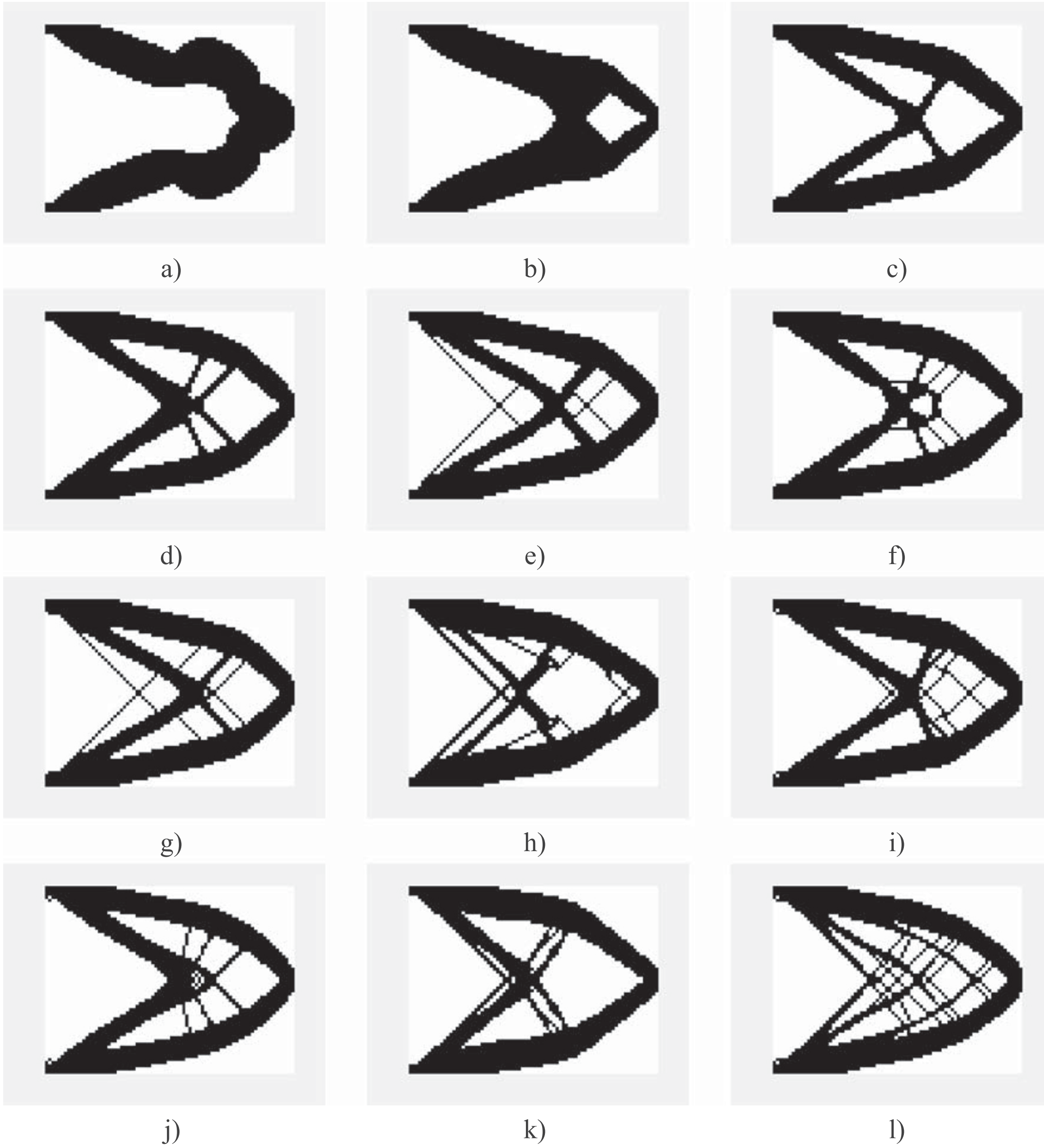

Fig. 7 Results of the HFM without controlling unit-area holes. The filter radius is equal to 1; the mesh comprises 80 × 60 unit square elements; and the maximum number of holes H is equal to 1, 2, 3, 5, 9, 11, 13, 17, 21, 29, 36, or 55. Here, h denotes the number of holes in the optimal structure. (**a**) H=1, h=0 (**b**) H=2, h=1 (**c**) H=3, h=3 (**d**) H=5, h=5 (**e**) H=9, h=9 (**f**) H=11, h=10 (**g**) H=13, h=11 (**h**) H=17, h=17 (**i**) H=21, h=20 (**j**) H=29, h=17 (**k**) H=36, h=18 (**l**) H=55, h=47

the condition that the area of the holes is not controlled (based on the topology optimization model in (2-a)). It shows that restricting the number of holes can alleviate the checkerboard pattern. However, when h increases, it is possible to appear the checkerboard pattern. Section 3.2 demonstrates the extended functionality of the HFM, which is to suppress checkerboard pattern, under the condition that the area of the holes is controlled (based on the topology optimization model in (2-b)). And we compare its results with those of the original BESO. Section 3.3 demonstrates the ability to use the HFM to mitigate the mesh dependence and checkerboard pattern phenomena (based on the topology optimization model in (2-b)).

A typical cantilever beam example is shown in Fig. 6, where the design domain is discretized with square elements and a unit load vector acts on a point in the middle of the right boundary of the design domain. Unless stated otherwise, the filter radius size r is set to a multiple of the unit length by default, and the unit length is equal to the edge length of the elements. The

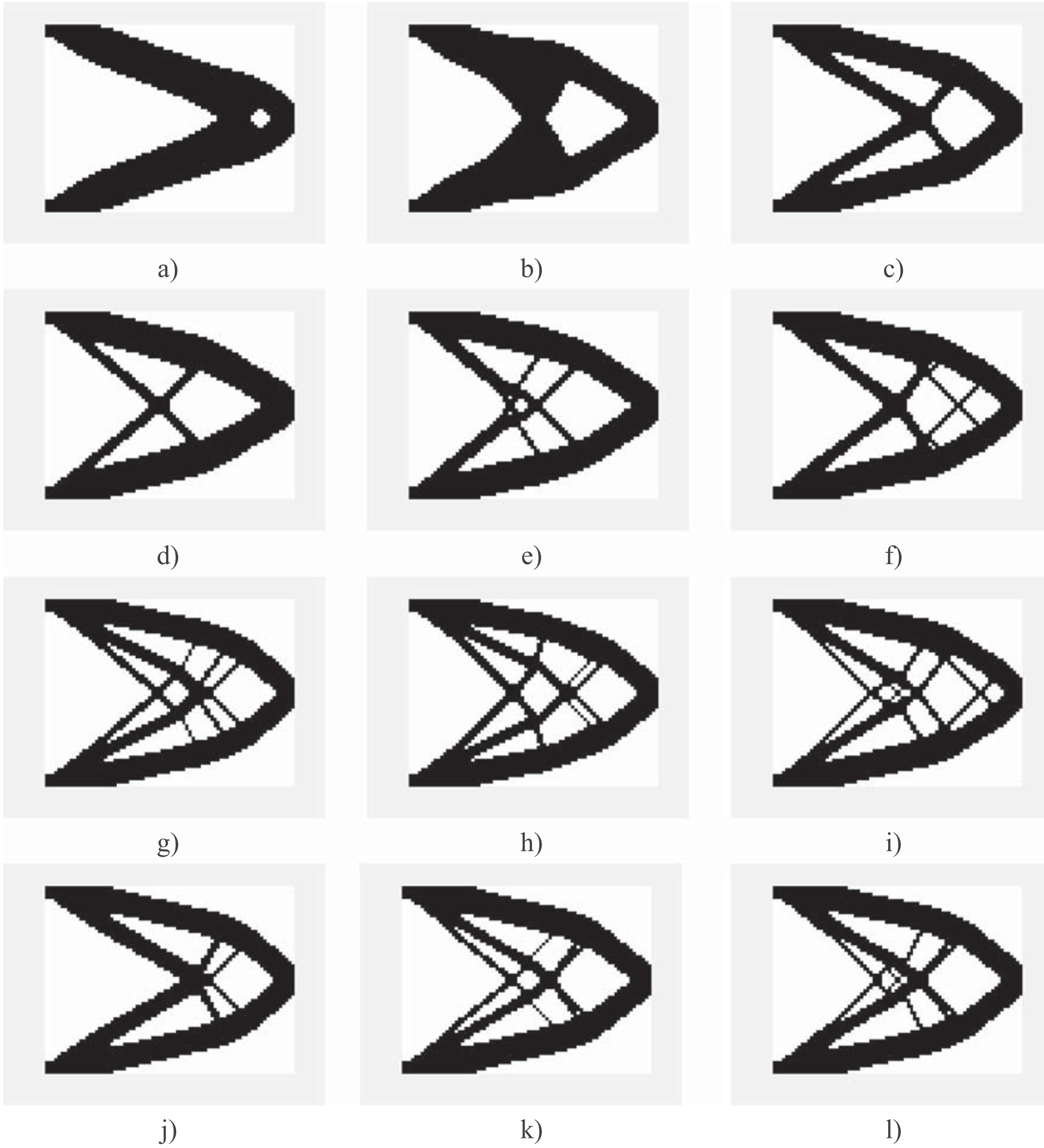

Fig. 8 Results of the HFM without controlling unit-area holes. The filter radius is equal to 1.2; the mesh comprises 80 × 60 unit square elements; and the maximum number of holes H is equal to 1, 2, 3, 5, 9, 11, 13, 17, 21, 29, 36, or 55. Here, h denotes the number of holes in the optimal structure. (**a**) H=1, h=1 (**b**) H=2, h=1 (**c**) H=3, h=3 (**d**) H=5, h=3 (**e**) H=9, h=8 (**f**) H=11, h=10 (**g**) H=13, h=12 (**h**) H=17, h=14 (**i**) H=21, h=16 (**j**) H=29, h=5 (**k**) H=36, h=12 (**l**) H=55, h=15

evolutionary volume ratio er is equal to 0.01, and the prescribed volume of the final structure is equal to 0.4.

3.1 Only the number of holes is controlled in the HFM

In this example, we deal with topology optimization problem as shown in (2-a), and the topological optimization problem is implemented with topological constraints via the HFM, where the mesh comprises 80 × 60 (xh × yv) unit square elements, and the allowed maximum number of holes H is 1, 2, 3, 5, 9, 11, 13, 17, 21, 29, 36, or 55. The optimized results without sensitivity filtering (filter radius equal to 1) and with sensitivity filtering (filter radius equal to 1.2) are shown in Figs. 7 and 8, respectively. Table 1 shows the numbers of holes in the

Table 1 Numbers of holes in the optimized results corresponding to Figs. 7 and 8

	H	1	2	3	5	9	11	13	17	21	29	36	55
Figure 7	h ($r = 1$)	0	1	3	5	9	10	11	17	20	17	18	47
Figure 8	h ($r = 1.2$)	1	1	3	3	8	10	12	14	16	5	12	15

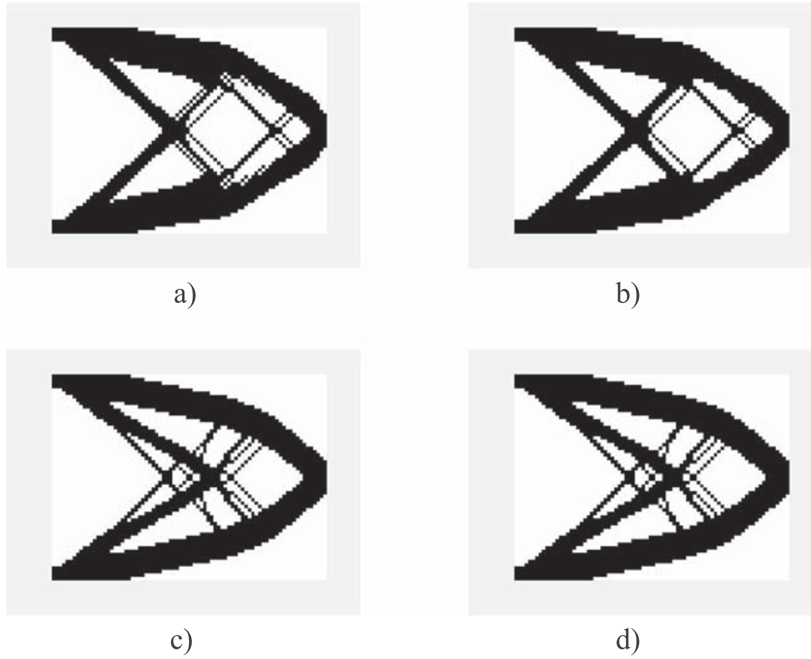

Fig. 9 **a, b** Results obtained **a** using the original BESO method and **b** by constraining the occurrence of unit-area holes ($S^* = 1$) in BESO with the HFM, with the filter radius equal to 1. **c,d** Results obtained **c** using the original BESO method and **d** by constraining the occurrence of unit-area holes ($S^* = 1$) in BESO with the HFM, with a filter radius equal to 1.2. For all examples, the mesh contains 80 × 60 unit square elements. (**a**) Original BESO mesh=80×60; r=1 (**b**) BESO with controling unit hole by HFM mesh=80×60; r=1 (**c**) Original BESO mesh=80×60; r=1.2 (**d**) BESO with controling unit hole by HFM mesh=80×60; r=1.2

optimized results. It is clearly shown that the HFM can work well under the constraint of a maximum allowed number of holes both with and without filtering.

3.2 Pictographic avoidance of the checkerboard pattern via the HFM

The checkerboard pattern in the 2D case can be heuristically seen from the presence of holes with an area equal to 1. According to the theory of the HFM, the checkerboard pattern phenomenon can be pictographically avoided by controlling the presence of unit-area holes. For this purpose, we deal with topology optimization problem as shown in (2-b) and compare its results with those of the original BESO.

As shown in Fig. 9, we tested the ability of the HFM to eliminate the checkerboard pattern by only filling in holes with an area equal to 1. Initially, the checkerboard pattern appears when no filter for sensitivity or density is used. This corresponds to the case in which the value of the filter radius is chosen to be 1 (see Fig. 9a). Usually, the checkerboard pattern can be suppressed by choosing a reasonably large value of the filter radius, such as 1.2, as shown in Fig. 9c; however, there

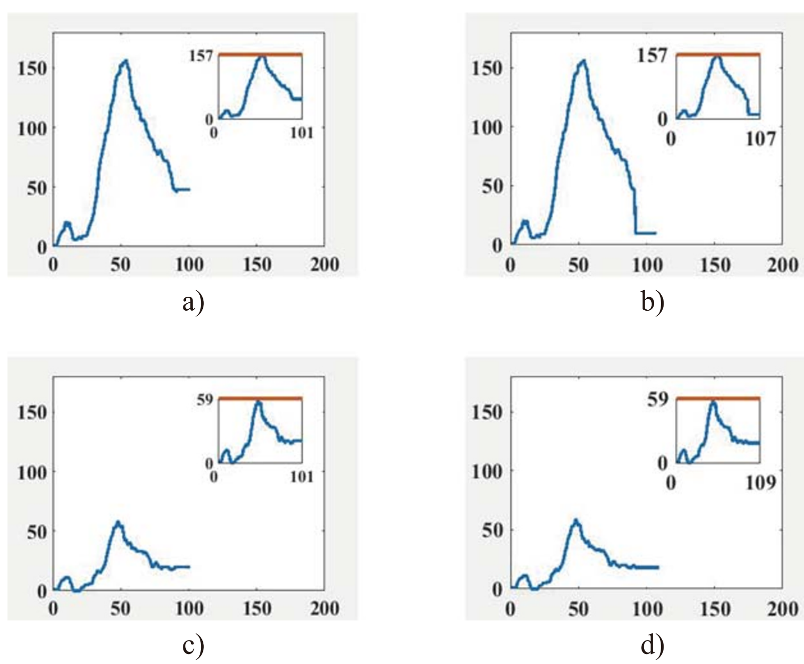

Fig. 10 History of the number of holes throughout the topological optimization process corresponding to the cases shown in Fig. 9. The vertical axis represents the number of holes calculated in real time after each iteration, and the horizontal axis represents the iteration number (**a**) Original BESO mesh=80×60; r=1 (**b**) BESO with controlling unit hole by HFM mesh=80×60; r=1 (**c**) Original BESO mesh=80×60; r=1.2 (**d**) BESO with controlling unit hole by HFM mesh=80×60; r=1.2

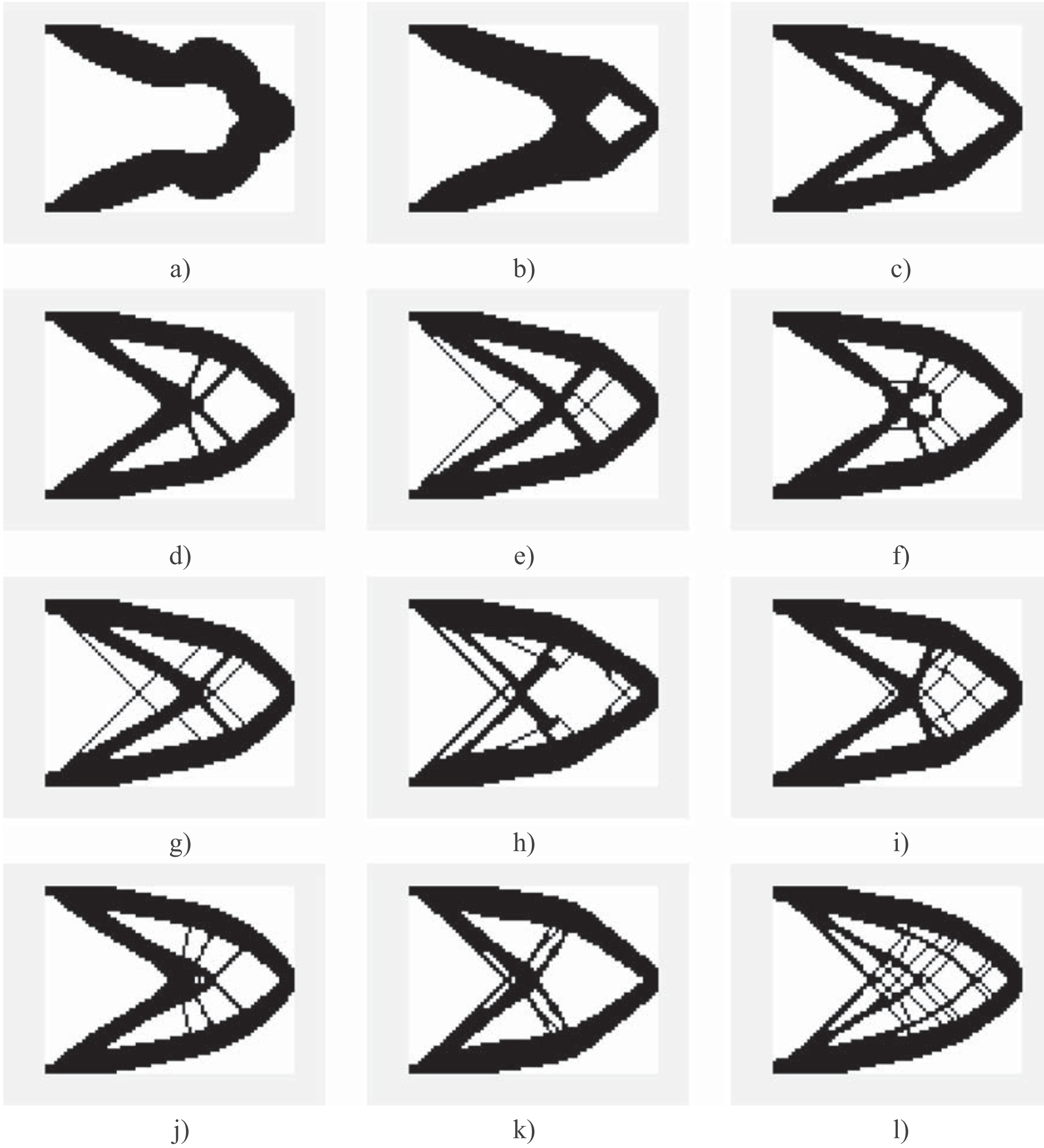

Fig. 11 Results of the HFM with $S^* = 1$ under the conditions that the filter radius is equal to 1, the mesh contains 80 × 60 elements, and the allowed maximum number of holes H is equal to 1, 2, 3, 5, 9, 11, 13, 17, 21, 29, 36, or 55. Here, h denotes the number of holes in the optimal structure (**a**) H=1, h=0 (**b**) H=2, h=1 (**c**) H=3, h=3 (**d**) H=5, h=5 (**e**) H=9, h=9 (**f**) H=11, h=10 (**g**) H=13, h=11 (**h**) H=17, h=13 (**i**) H=21, h=16 (**j**) H=29, h=9 (**k**) H=36, h=10 (**l**) H=55, h=35

may exist several holes with an area equal to 1 even when using sensitivity filtering. Straightforwardly, a filter with a sufficiently large radius will suppress the checkerboard pattern completely, but this may also change the optimized topology by smearing out thin parts of the structure during the optimization procedure.

Under condition that the HFM is only used to fill in holes with an area equal to 1, as shown in Fig. 9 b and d (which present the optimized results without and with filtering, corresponding to filter radii of 1 and 1.2, respectively), the value of H can be chosen to be much larger than the maximum number of holes that appear during the optimization process in standard soft-kill BESO (e.g., H = 200 is much larger than the peak numbers of holes seen in Fig. 10a and c, which are 59 and 157, respectively), meaning that the constraint $h \leq H$ is always satisfied throughout the whole optimization process. Figure 11 presents the results of a test of the ability of the HFM to pictographically suppress the checkerboard pattern under the conditions that the mesh is fixed and the number of holes is controlled.

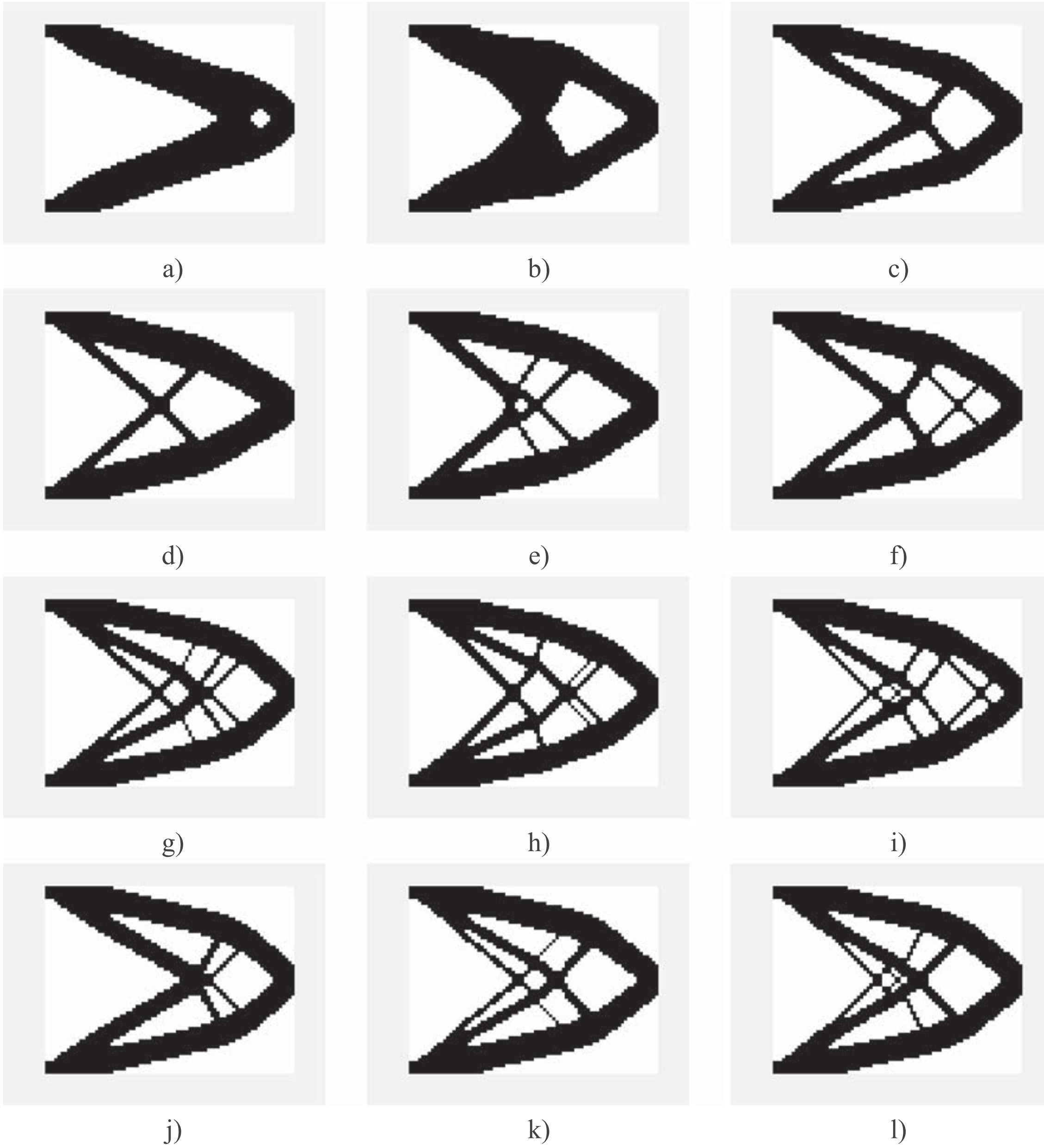

Fig. 12 Results of the HFM with $S^* = 1$. The filter radius is equal to 1.2; the mesh comprises 80×60 unit square elements; and the maximum number of holes H is equal to 1, 2, 3, 5, 9, 11, 13, 17, 21, 29, 36, or 55. Here, h denotes the number of holes in the optimal structure. **a** H=1, h=1 **b** H=2, h=1 **c** H=3, h=3 **d** H=5, h=3 **e** H=9, h=6 **f** H=11, h=6 **g** H=13, h=10 **h** H=17, h=10 **i** H=21, h=14 **j** H=29, h=5 **k** H=36, h=8 **l** H=55, h=11

Figure 11 corresponds to an example of a cantilever beam, as shown in Fig. 6, where the design domain consists of 80×60 square elements and the filter radius is equal to 1. The checkerboard pattern appears in Fig. 9a, which shows the result obtained using the original BESO method under the same conditions; by contrast, the results in Fig. 11 are obtained using the HFM with the maximum number of holes H set equal to 1, 2, 3, 5, 9, 11, 13, 17, 21, 29, 36, or 55. By controlling the occurrence of unit-area holes, the checkerboard pattern is pictographically suppressed. However, while some of the optimal structures have a reasonable topology, others do not. These findings reveal that even if the checkerboard pattern can be pictographically suppressed, the reasonability of the optimized structure might not be guaranteed merely by using the HFM.

Figure 12 shows more reasonable design results obtained via a combination of sensitivity filtering and the HFM with control of the occurrence of unit-area holes. Table 2 lists the numbers of holes in the optimized

Table 2 Numbers of holes in the optimized results corresponding to Figs. 11 and 12

	H	1	2	3	5	9	11	13	17	21	29	36	55
Figure 11	h ($r=1$)	0	1	3	5	9	10	11	13	16	9	10	35
Figure 12	h ($r=1.2$)	1	1	3	3	6	6	10	10	14	5	8	11

results for each corresponding allowed maximum number of holes H. Figure 13 illustrates the topological optimization processes of the HFM corresponding to Fig. 12. Figure 13 shows how the number of holes varies with the iteration number during topological optimization.

3.3 Test of using the HFM to mitigate the mesh dependence and checkerboard pattern phenomena

In this section, we test of using the HFM to mitigate the mesh dependence and checkerboard pattern phenomena based on the topology optimization model in (2-b).

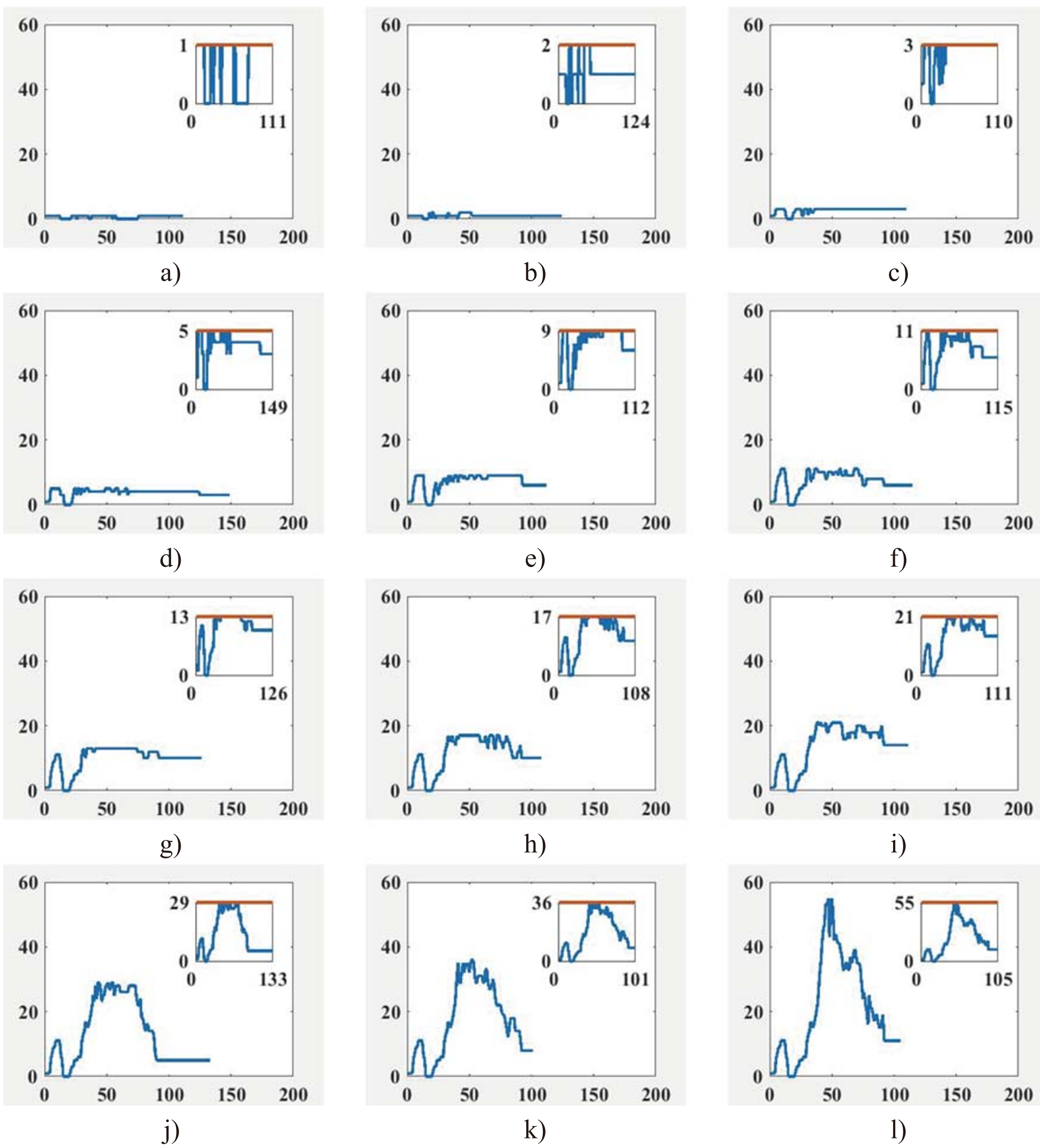

Fig. 13 History of the number of holes in each iteration of topology optimization corresponding to Fig. 12. The vertical axis represents the number of holes calculated in real time after each iteration, and the horizontal axis represents the iteration number. **a** H=1, h=1 **b** H=2, h=1 **c** H=3, h=3 **d** H=5, h=3 **e** H=9, h=6 **f** H=11, h=6 **g** H=13, h=10 **h** H=17, h=10 **i** H=21, h=14 **j** H=29, h=5 **k** H=36, h=8 **l** H=55, h=11

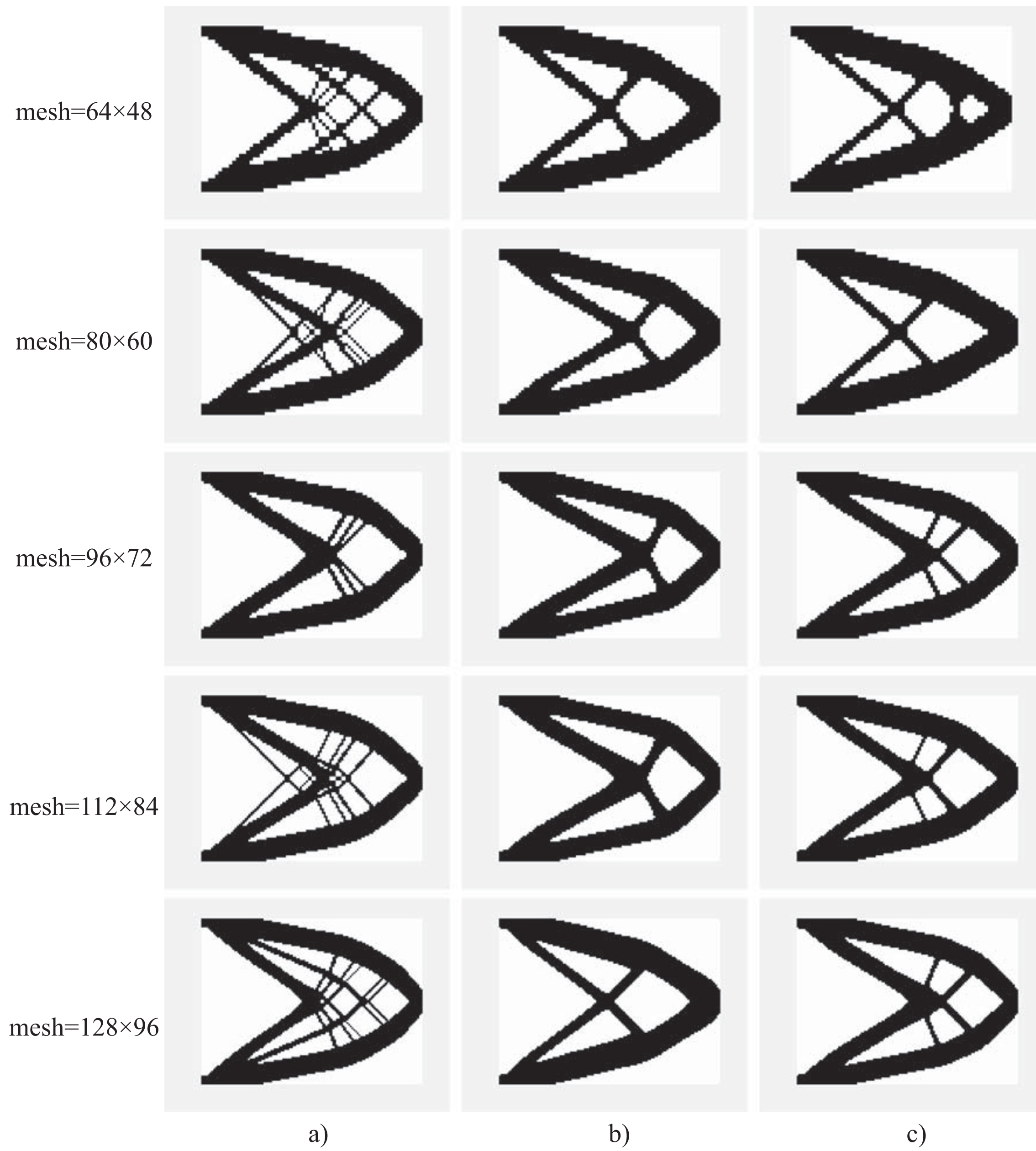

Fig. 14 Results of **a** the original BESO method and **b,c** the HFM with $S^* = 1$, where the filter radius is equal to 1.2 and the mesh contains 64×48, 80×60, 96×72, 112×84, or 128×96 unit square elements. The allowed maximum number of holes H is equal to 3 in (**b**) and 5 in (**c**). **a** Original BESO **b** H=3 **c** H=5

3.3.1 Examples of the HFM under the condition of a fixed filter radius

Figure 14a shows how the number of holes in the optimized structure obtained using the original BESO method differs when the filter radius is 1.2 and the mesh dimensions are 64×48, 80×60, 96×72, 112×84, and 128×96. This well-known phenomenon is referred to as mesh dependence. Figure 14b and c show that the HFM can limit the changes to the topology under different mesh discretizations. In particular, the mesh dependence can be limited by imposing a stringent constraint on the allowed maximum number of holes, such as $H = 3$. When the allowed maximum number of holes H increases, the topology of the structure changes within a certain range, such as $H = 5$. Figure 15 shows the history of the number of holes throughout each topology optimization process corresponding to Fig. 14.

Figure 16 shows the capabilities of the HFM without sensitivity filtering. The checkerboard pattern and mesh dependence phenomena can be simultaneously limited by imposing a rigorous constraint on the allowed maximum number of holes, such as $H = 3$. When the allowed maximum number

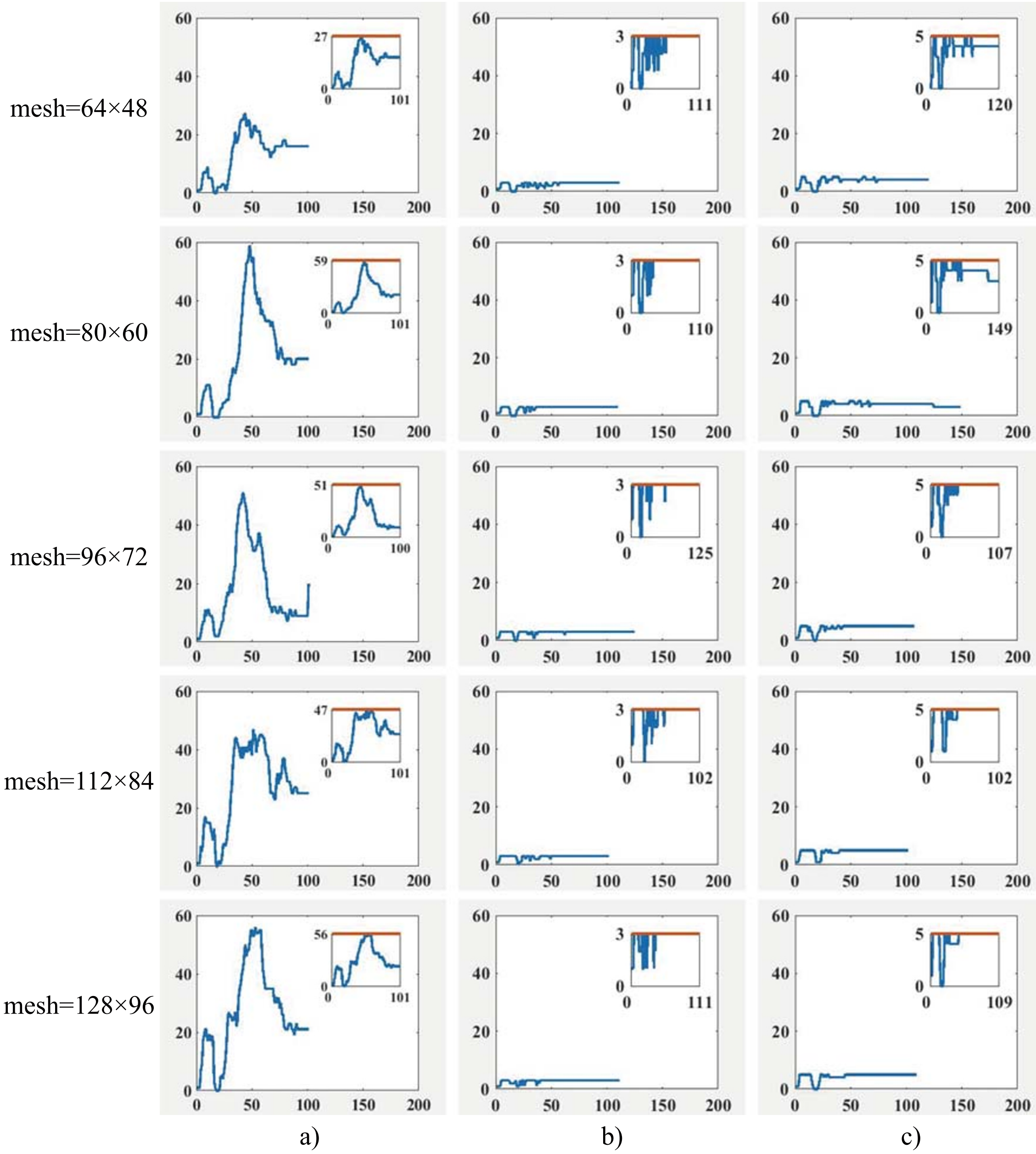

Fig. 15 History of the number of holes in each iteration of topology optimization corresponding to Fig. 14. The vertical axis represents the number of holes calculated in real time after each iteration, and the horizontal axis represents the iteration number. **a** Original BESO **b** H=3 **c** H=5

of holes H = 5, the topology of the structure has changed within a certain range h ≤ 5.

3.3.2 Examples of the HFM under the condition that the filter radius is defined by a fixed scaling factor

The phenomenon of mesh dependence can be partially mitigated by choosing a fixed scaling factor. Figures 17a and 18a show the performance of the standard BESO method with different filter radii but a fixed scaling factor for the filter radius. Figures 17b and c and 18b and c show the performance of the HFM with the filter radius when H is chosen to be 3 and 5, respectively.

From Fig. 16c (mesh = 112 × 84), Fig. 17c (mesh = 72 × 54), and Fig. 18c (mesh = 88 × 66), we can observe that very thin branches exist in the optimized topologies even with a small upper bound H on the allowed number of holes. The HFM can only be used to adjust the number of holes (void subdomain) in the optimized structure. Therefore, the HFM cannot directly control the minimal characteristic size of the structure (solid subdomain). Instead, a sensitivity filter with a reasonable radius should be applied as an effective method to filter out very thin

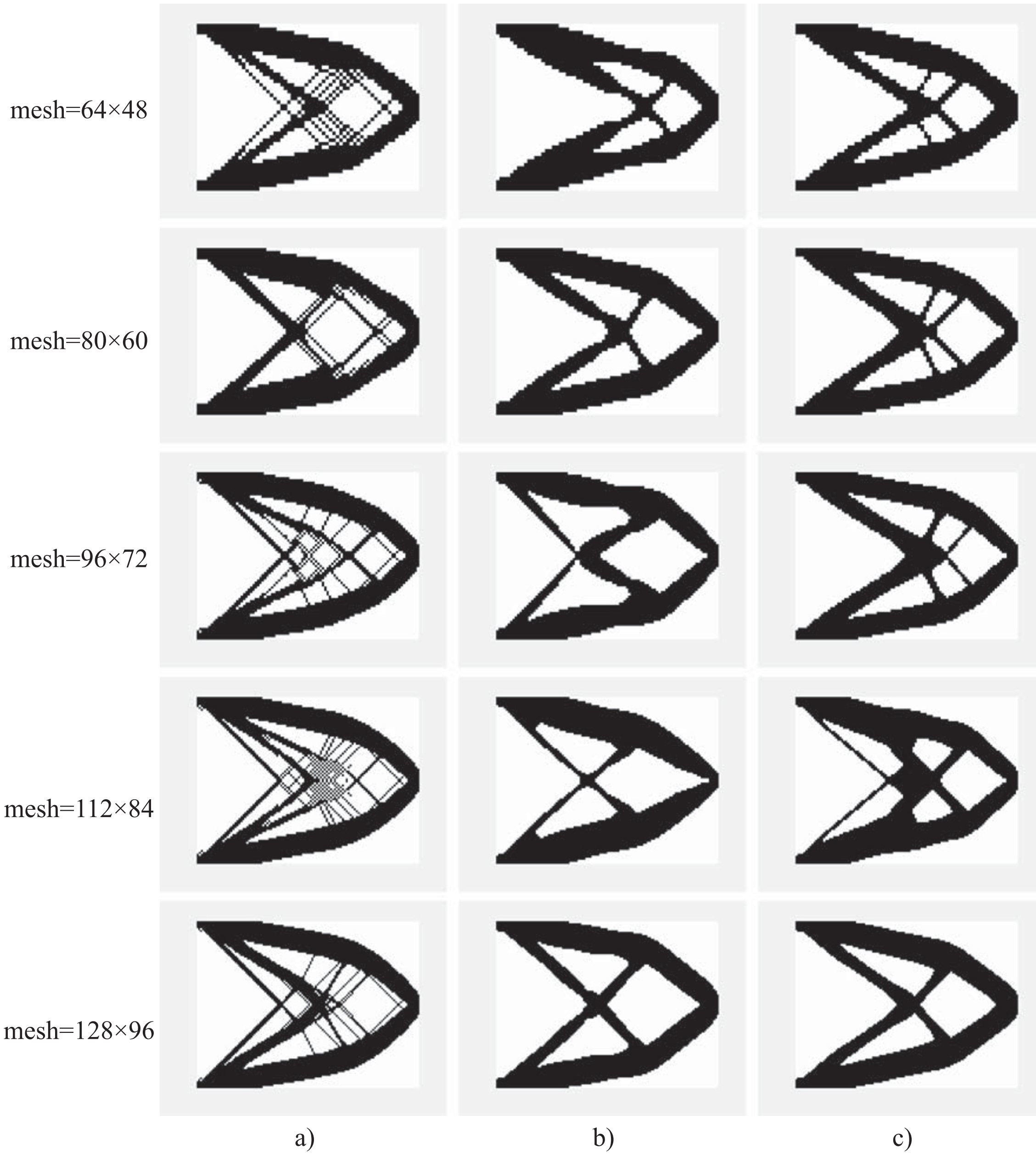

Fig. 16 Results of **a** the original BESO method and **b,c** the HFM with $S^* = 1$ under the conditions that the filter radius is equal to 1; the mesh contains 64×48, 80×60, 96×72, 112×84, or 128×96 (xh×yv) elements; and the allowed maximum number of holes H is equal to 3 or 5. **a** Original BESO **b** H=3 **c** H=5

branches in the optimal structure. In addition to the filtering methods, we also recommend using the minimum size control method (Yang et al. 2019, Zhou et al. 2015) to suppress the production of very thin branches in optimal structure.

4 Discussion

In this paper, we have proposed the HFM as a method of filling in holes when the number of holes in an optimized topological structure exceeds the constraint on the allowed maximum number of holes. The algorithm checks the number of holes in the structure and chooses which hole will be filled. Based on the working principle of the HFM, the user can specify that holes with a specific area should be filled in (such as holes of unit area, as done in this paper) and diverse other approaches. For example, we can order the sequence of holes based on the hole area during the topological optimization process. When the number of holes is greater than the allowed maximum number of holes H, the holes will be filled in order from smallest to largest

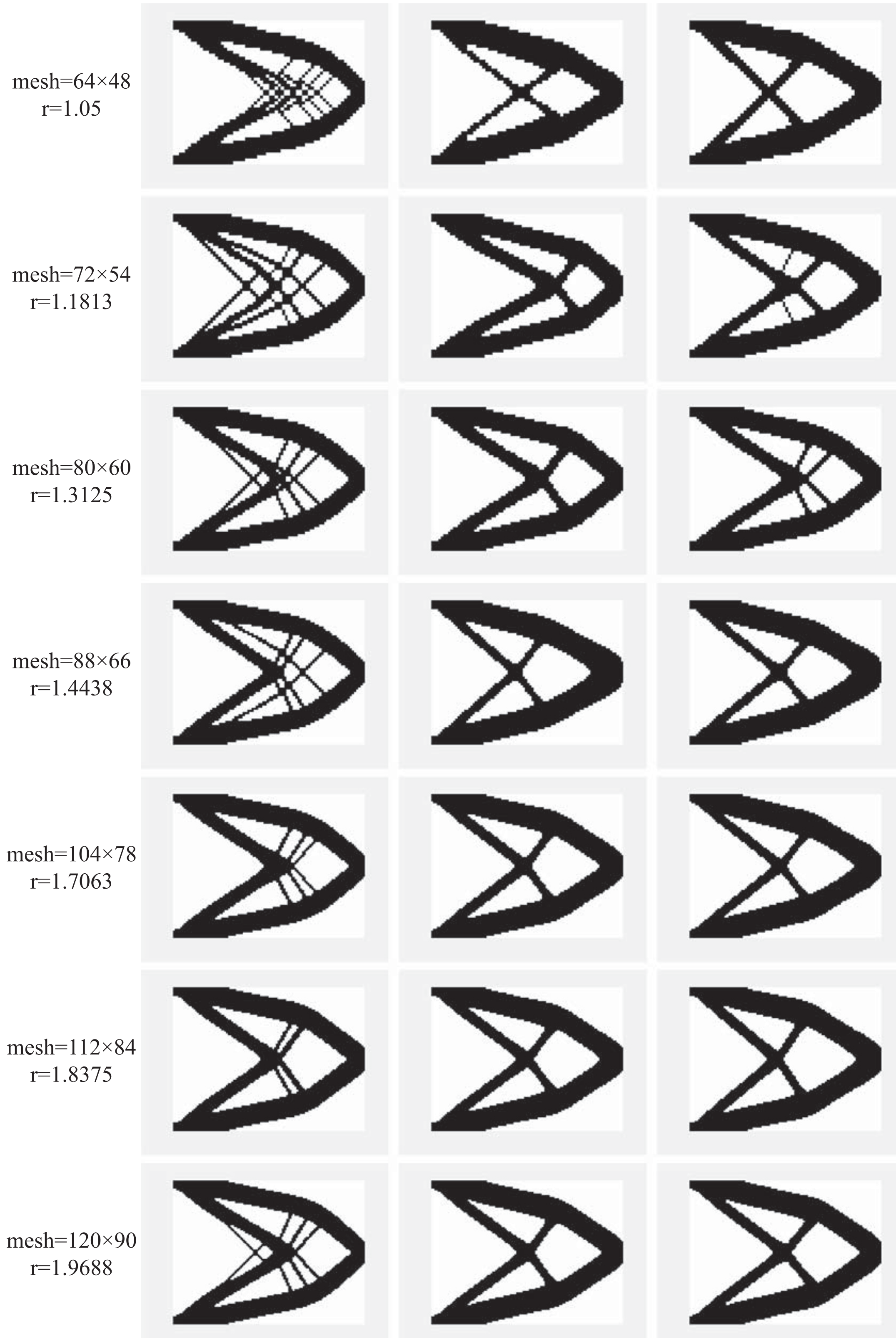

a) b) c)

Fig. 17 Results of **a** the original BESO method and **b,c** the HFM with $S^* = 1$, when the allowed maximum number of holes is **b** H = 3 and **c** H = 5, with different mesh sizes. The filter radius is defined by a scaling factor of 21/1280 relative to the length of the horizontal side of the design domain

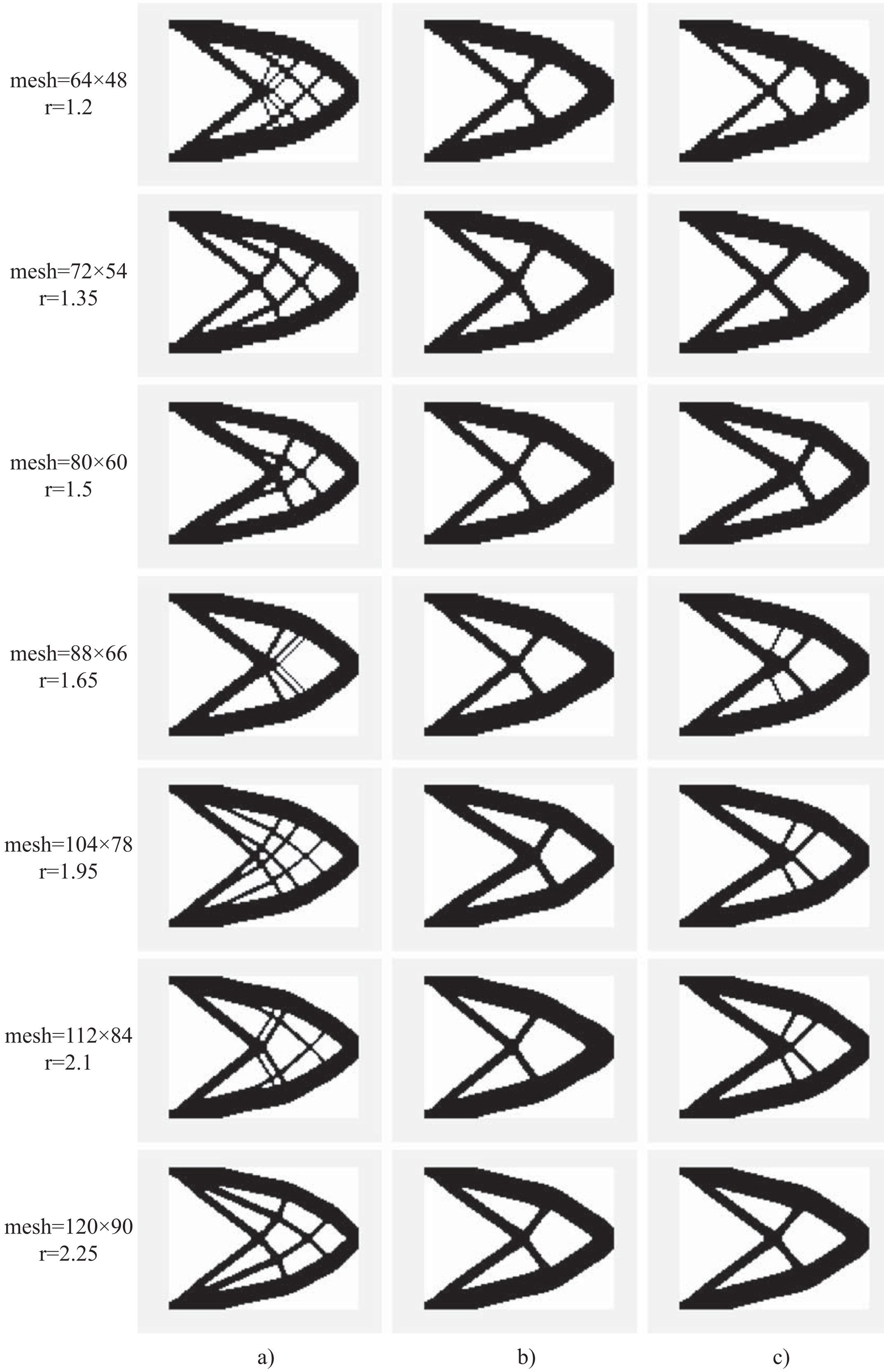

Fig. 18 Results of **a** the original BESO method and **b,c** the HFM with $S^* = 1$, when the allowed maximum number of holes is **b** $H = 3$ and **c** $H = 5$, with different mesh sizes. The filter radius is defined by a scaling factor of 3/160 relative to the length of the horizontal side of the design domain

until the constraint on the number of holes is satisfied. Through this method, we can indirectly avoid an optimized topology with many tiny holes. However, this method alone cannot guarantee a reasonable solution.

The BESO method has the feature that the solution is binarized in each iteration of topology optimization. To enable the use of the HFM, as shown in this paper, it might also be necessary to binarize the design variables in each iteration of the SIMP method. Therefore, if we can present a unified criterion for binarizing the design variables that is also compatible with the SIMP method, the HFM can also be used to constrain the number of holes for SIMP optimization.

The numerical instability phenomenon of mesh dependence can be mitigated under the condition that the maximum number of holes H is set to an appropriately small value. Numerical examples also show that if an appropriately large filter radius is chosen, then the HFM can suppress the mesh dependence within a wide range of the maximum number of holes H.

Based on the numerical examples presented in Section 3, it seems that an excessively stringent constraint on the allowed maximum number of holes, such as $H < 3$, will result in poor convergence. The results also suggest that the allowed maximum number of holes H should be chosen to be a reasonably large value at the beginning of optimization and then decreased during the optimization procedure. If the initial constraints are too tight, the optimization may converge to a poor solution.

Since both the digital Gauss-Bonnet formulation, which is used to calculate the number of holes (or handles, in 3D), and the burning method, which is used to calculate the areas of the holes (or the volumes of voids), can also be implemented for a 3D structure, the proposed HFM for the 2D case can optimistically be extended to the 3D case. Such an extension deserves considerable further research work to determine the implementation details.

5 Conclusion

The HFM based on the soft-kill BESO method is proposed to achieve structural topology optimization while strictly satisfying an inequality constraint on the allowed maximum number of holes throughout the whole optimization procedure. The HFM can pictographically suppress the checkerboard pattern phenomenon under the constraint that the area of any hole must be larger than 1 ($S^* = 1$ in (2-b)). The mesh dependence phenomenon can be mitigated by imposing a very tight constraint on the allowed maximum number of holes. Numerical examples reveal that the performance of the HFM is reliable. Based on these features, even a practitioner who is not familiar with topology optimization can use the HFM in combination with filtering to directly limit the complexity of the topology of an optimized structure. The current implementation of the HFM for use in combination with an optimization algorithm is limited to the benchmark case of performing a two-dimensional optimization of a structure while minimizing its compliance. The extension of the current version of the HFM to corresponding benchmark examples in three dimensions will be more challenging and will be further studied in the future.

Acknowledgments The authors are grateful to Yimin Xie and Xiaodong Huang for providing the MATLAB codes for BESO. The authors thank Prof. Xianfeng David Gu (Stony Brook University) for valuable discussions about algebra topology.

Funding This research was funded by the National Science Foundation of China under grant no. 51675506 and under National Science and Technology Major Project 2017ZX10304403.

Compliance with ethical standards

Conflict of interest The authors declare that they have no conflict of interest.

Replication of results The original Soft-BESO MATLAB code by Yimin Xie and Xiaodong Huang can be downloaded at http://www.isg.rmit.edu.au.

The results presented in Section 3 were obtained via the HFM using a MATLAB function defined as follows:

Soft_BESO_HFM (xh, yv, V, r, er, H, flag).

The complete MATLAB code is given as an Appendix file.

Nomenclature A_1, The set consisting of all elements of a connected structure; A_i, The i-th set of solid elements that belong to a connected structure; b_1, A solid element; B, The set of solid elements; c, The optimization objective; C, The set consisting of solid elements connected by an edge to b_1 or an element of D; D, The set consisting of solid elements included in both C and B; er, The evolutionary volume ratio; E_1, The Young's modulus of the solid material; $\mathbf{F}$, The force vectors; g, The number of holes in the connected structure; G, The cell consisting of holes in order of area size from largest to smallest, consisting of finite elements; G_j, The hole at the j-th position in G; h, The number of holes in the topological structure in each iteration; $h0$, The peak value of the number of holes during the topology optimization process; H, The allowed maximum number of holes in the optimal structure as defined by the user; $\mathbf{k_0}$, The element stiffness matrix for an element with unit Young's modulus; $\mathbf{K}$, The global stiffness matrix; M_i, (i = 4, 2) The set of digital points with i neighboring edges; n, The number of connected structures in the current iteration of topology optimization; N, The number of elements used to discretize the design domain; p, The penalization power; r, The filter radius, relative to the unit length; S_i, The area of the i-th hole; S^*, A prescribed minimum area of the hole in final structure. In this paper, we set $S^* = 1$; $\mathbf{u_e}$, The element displacement vector; $\mathbf{U}$, The global displacement; VA_1, The set consisting of void elements connected to each other by an edge; VA, The cell consisting of void elements, where each element of VA is a hole; vb_1, A void element; VB, The set consisting of all void elements; VC, The set consisting of void elements connected by an edge to a void element of VD or vb_1; VD, The set consisting of void elements included in both VC and VB; V_e, The volume of an individual element; V^*, The prescribed volume of the final structure; xh, The numbers of elements in the horizontal direction of design domain; yv, The numbers of elements in the vertical direction of design domain; $\boldsymbol{\rho}$, The design variables; ρ_e, The design variable of the e-th element; ρ_{min}, A fixed value equal to 0.001

References

Andreassen E, Clausen A, Schevenels M, Lazarov B, Sigmund O (2011) Efficient topology optimization in MATLAB using 88 lines of code. Struct Multidiscip Optim 43:1–16. https://doi.org/10.1007/s00158-010-0594-7

BendsØe MP, Sigmund O (1999) Material interpolation schemes in topology optimization. Arch Appl Mech 69:635–654. https://doi.org/10.1007/s004190050248

BendsØe MP (1989) Optimal shape design as a material distribution problem. Struct Optim 1:193–202. https://doi.org/10.1007/BF01650949

Bourdin B (2001) Filters in topology optimization. Int J Numer Methods Eng 50:2143–2158. https://doi.org/10.1002/nme.116

Borrvall T, Petersson J (2003) Topology optimization of fluids in stokes flow. Int J Numer Methods Fluids 41:77–107. https://doi.org/10.1002/fld.426

Buhl T, Pedersen CBW, Sigmund O (2000) Stiffness design of geometrically nonlinear structures using topology optimization. Struct Multidiscip Optim 19:93–104. https://doi.org/10.1007/s001580050089

Chen SK, Chen W, Lee SH (2010) Level set based robust shape and topology optimization under random field uncertainties. Struct Multidiscip Optim 41:507–524. https://doi.org/10.1007/s00158-009-0449-2

Chen L, Rong Y (2010) Digital topological method for computing genus and the Betti numbers. Topol Appl 157(12):1931–1936. https://doi.org/10.1016/j.topol.2010.04.006

Chen L (2004) Discrete surfaces and manifolds. Sp Computing, Rockville

Deng Y, Korvink JG (2018) Self-consistent adjoint analysis for topology optimization of electromagnetic waves. J Comput Phys 361:353–376. https://doi.org/10.1016/j.jcp.2018.01.045

Deng Y, Liu Z, Zhang P, Liu Y, Wu Y (2011) Topology optimization of unsteady incompressible Navier_Stokes flows. J Comput Phys 230:6688–6708. https://doi.org/10.1016/j.jcp.2011.05.004

Evgrafov A, Pingen G, Maute K (2008) Topology optimization of fluid domains: kinetic theory approach. ZAMM 88:129–141. https://doi.org/10.1002/zamm.200700122

Gu DX, Yau ST (2008) Computational conformal geometry. HIGHER EDUCATION PRESS. International Press, Somerville, Massachusetts, U.S.A.; Higher Education Press, Beijing, China

Gersborg-Hansen A, Sigmund O, Haber RB (2005) Topology optimization of channel flow problems. Struct Multidiscip Optim 20:181–192. https://doi.org/10.1007/s00158-004-0508-7

Guest JK, Prevost JH, Belytschko T (2004) Achieving minimum length scale in topology optimization using nodal design variables and projection functions. Int J Numer Methods Eng 61:238–254. https://doi.org/10.1002/nme.1064

Huang X, Xie YM (2009) Bi-directional evolutionary topology optimization of continuum structures with one or multiple materials. Comput Mech 43:393–401. https://doi.org/10.1007/s00466-008-0312-0

Lazarov BS, Sigmund O (2011) Filters in topology optimization based on Helmholtz-type differential equations. Int J Numer Methods Eng 86:765–781. https://doi.org/10.1002/nme.3072

Lazarov BS, Wang FW, Sigmund O (2016) Length scale and manufacturability in density-based topology optimization. Arch Appl Mech 86:189–218. https://doi.org/10.1007/s00419-015-1106-4

Labbe T, Dehez B (2011) Topology optimization method based on the Maxwell stress tensor for the design of ferromagnetic parts in electromagnetic actuators. IEEE Trans Magn 47:2188–2193. https://doi.org/10.1109/TMAG.2011.2138151

Mlejnek HP (1992) Some aspects of the genesis of structures. Struct Optim 5:64–69. https://doi.org/10.1007/BF01744697

Okamoto Y, Wakao S, Sato S (2016) Topology optimization based on regularized level-set function for solving 3-D nonlinear magnetic field system with spatial symmetric condition. IEEE Trans Magn 52:3. https://doi.org/10.1109/tmag.2015.2492978

Osher S, Sethian JA (1988) Fronts propagating with curvature dependent speed: algorithms based on Hamilton-Jacobi formulations. J Comput Phys 79:12–49. https://doi.org/10.1016/0021-9991(88)90002-2

Rozvany GIN (2001) Aims, scope, methods, history and unified terminology of computer-aided topology optimization in structural mechanics. Struct Multidiscip Optim 21:92–108. https://doi.org/10.1007/s001580050174

Rozvany GIN (2009) A critical review of established methods of structural topology optimization. Struct Multidiscip Optim 37:217–237. https://doi.org/10.1007/s00158-007-0217-0

Sigmund O (2009) Manufacturing tolerant topology optimization. Acta Mech Sinica 25:227–239. https://doi.org/10.1007/s10409-009-0240-z

Sigmund O (2001a) Design of multiphysics actuators using topology optimization - part I: one-material structures. Comput Methods Appl Mech Eng 190:6577–6604. https://doi.org/10.1016/S0045-7825(01)00251-1

Sigmund O (2001b) Design of multiphysics actuators using topology optimization - part II: two-material structures. Comput Methods Appl Mech Eng 190:6605–6627. https://doi.org/10.1016/S0045-7825(01)00252-3

Sigmund O (2001c) A 99 line topology optimization code written in Matlab. Struct Multidiscip Optim 21:120–127. https://doi.org/10.1007/s001580050176

Sigmund O, Petersson J (1998) Numerical instabilities in topology optimization: a survey on procedures dealing with checkerboards, mesh-dependencies and local minima. Struct Optim 16:68–75. https://doi.org/10.1007/BF01214002

Sigmund O (2007) Morphology-based black and white filters for topology optimization. Struct Multidiscip Optim 33:401–424. https://doi.org/10.1007/s00158-006-0087-x

Talischi C, Paulino GH, Pereira A, Menezes IFM (2012) PolyMesher: a general-purpose mesh generator for polygonal elements written in Matlab. Struct Multidiscip Optim 45:309–328. https://doi.org/10.1007/s00158-011-0706-z

Wang F, Lazarov BS, Sigmund O (2011) On projection methods, convergence and robust formulations in topology optimization. Struct Multidiscip Optim 43:767–784. https://doi.org/10.1007/s00158-010-0602-y

Xie YM, Steven GP (1992) A simple evolutionary procedure for structural optimization. Comput Struct 49(5):885–896. https://doi.org/10.1016/0045-7949(93)90035-C

Xie YM, Steven GP (1997) Evolutionary structural optimization. Springer, London

Yamada T, Izui K, Nishiwaki S (2010) A topology optimization method based on the level set method incorporating a fictitious interface energy. Comput Methods Appl Mech Eng 199:2876–2891. https://doi.org/10.1016/j.cma.2010.05.013

Yang KK, Fernandez E, Cao N, Duysinx P, Zhu JH, Zhang W (2019) Note on spatial gradient operators and gradient-based minimum length constraints in SIMP topology optimization. Struct

Multidiscip Optim 60:393–400. https://doi.org/10.1007/s00158-019-02269-9

Zuo WJ, Saitou K (2017) Multi-material topology optimization using ordered SIMP interpolation. Struct Multidiscip Optim 55:477–491. https://doi.org/10.1007/s00158-016-1513-3

Zhou M, Rozvany GIN (1991) The COC algorithm, part II: topological, geometry and generalized shape optimization. Comp Meth Appl Mech Engrng 89:197–224. https://doi.org/10.1016/0045-7825(91)90046-9

Zhou MD, Lazarov BS, Wang FW, Sigmund O (2015) Minimum length scale in topology optimization by geometric constraints. Comput Methods Appl Mech Eng S0045-7825(15):00169–00163. https://doi.org/10.1016/j.cma.2015.05.003